Spectroscopic characterization of exoplanets : from LOUPE to SINFONI

Hoeijmakers, H.J.

1 INTRODUCTION

1.1 THE SEARCH FOR EXTRA-SOLAR PLANETS

1.1.1 *Introduction*

Speculations and ideas about the existence of planets in solar systems other than our own can be traced through the scientific and popular literature to decades before the discovery of the first extra-solar planets (*exoplanets*). The first discovery of a planetary mass object outside the solar system was made in 1992, orbiting the pulsar PSR1257+12 (Wolszczan et al., 1992). This object lives in the extreme radiation environment of the pulsar and is believed to have formed from the remnants of the debris disk that that may have formed after the supernova explosion of the progenitor star (Miller et al., 2001; Hansen et al., 2009; Kerr et al., 2015). The discovery of the first exoplanet around a main sequence star is attributed to Mayor et al. (1995), who discovered a planet orbiting around the sun-like star 51 Pegasi in 1995. This planet was discovered via the periodic motion of the star induced by the gravitational pull of the planet. Many times in astronomy, observations are biased towards the most extreme kinds of objects, which are discovered first because they are the easiest to detect. This is certainly true for the detection of the first exoplanets: 51 Pegasi b is a gas giant half as massive as Jupiter, but orbits its star at a distance of 0.052 AU, completing one revolution every 4.2 days (Mayor et al., 1995; Butler et al., 2006; Brogi et al., 2013; Birkby et al., 2017). This planet could be detected because its gravitational influence on the star is relatively large due to its small orbital distance. The gravitational interaction between the planet and the star also induces strong tidal forces that act to circularize the orbit of the planet and synchronize the axial (diurnal) rotation period with the orbital period. The likely consequence is that one hemisphere of the planet always faces the scorching radiation of the nearby star and is heated to temperatures of over 1000 Kelvin, while the other side of the planet perpetually faces towards outer space (Brogi et al., 2013). Clearly, this planet is unlike any of the planets in the solar system, which is why its unexpected discovery has had an enormous impact.

51 Pegasi b was the first of a new class of exoplanets that are nowadays referred to as *hot Jupiters* (see Figure 1.1). Via numerous exoplanet-finding surveys, many planets like it have been discovered since. However as surveys have become more sensitive to smaller and cooler planets, it has become clear that hot Jupiters actually form a small minority in a much larger, di-

verse exoplanet population. At the time of writing, over 3600 planets have been discovered and have been independently followed-up[1]. These planets occupy a broad parameter space, and include rocky planets as well as gas giants orbiting various types of stars over a wide range of orbital distances. Although this entire population has not yet fully been explored, there does not seem to be an indication that any system can be considered to be typical.

Theories of how planets form must explain this diversity in the exoplanet population, including extreme examples like hot Jupiters. 22 years after the discovery of the first exoplanets, the mechanism of planet formation is still not fully understood. Proposed planet formation theories broadly fall into three categories:

1. The core-accretion model (Pollack et al., 1996) describes the gradual coagulation of dust particles into a proto-planetary core, which gravitationally attracts more particles as it grows. When sufficiently massive, it rapidly accretes gas in a runaway fashion until the star-forming disk is cleared by the onset of nuclear fusion in the core of the newborn star.

2. The disk gravitational instability model (Boss, 1997) posits that planets may form from self-gravitating clumps of disk material that are created by dynamical instabilities in the disk.

3. The pre-stellar nebula may fragment into separate clumps at an early stage, in which planets may form in a similar way as binary stars albeit with extreme mass ratios (see e.g. Hennebelle et al., 2008).

It is possible that all these formation pathways take place in nature to some degree. Identifying the dominant formation process then requires the careful study of both planet-forming disks as well as exoplanets themselves, because the present-day state of an exoplanet may in part be determined by its formation scenario (Madhusudhan et al., 2014).

An important factor in all three formation pathways is *planet migration*: During the formative stages the orbit of the planet may evolve, causing it to migrate inwards or outwards. Migration may be caused by the interplay between the planet and the disk material in which it is formed, gravitational interactions with other planets in the system, tidal interactions with the star and stellar encounters (Rasio et al., 1996; Weidenschilling et al., 1996; Ward, 1997; Laughlin et al., 1998; Ida et al., 2000). If a planet retains its primordial atmosphere, its present-day chemical composition may be indicative of its formation environment and therefore shed light on its migration history (Öberg et al., 2011). The realization that planet migration is an important aspect of planet formation has also influenced the way we understand our own solar

1 Exoplanet.eu maintains a database of exoplanet discoveries and candidates (Schneider et al., 2011)

system. It is now suspected that the planets in our solar system underwent some form of migration during their formation, which could help to explain phenomena like the peculiar axial tilt of Uranus and Venus, the catastrophic impact that may have been responsible for the formation of the Moon, the Late Heavy Bombardment and the presence and distribution of planetesimals in the solar system (Thommes et al., 1999; Gomes et al., 2005; Tsiganis et al., 2005; Levison et al., 2008). The study of exoplanets therefore informs existential questions about the solar system, the Earth and the origins of life.

The discovery of a diverse exoplanet population concerns another major question that has insisted on humanity since the dawn of astronomy: *Does life exist on planets elsewhere in the universe?* When overall size and mass are considered, there are many planets that resemble the Earth (a.o. see Petigura et al., 2013; Foreman-Mackey et al., 2014; Silburt et al., 2015; Burke et al., 2015; Coughlin et al., 2016; Kane et al., 2016). A fraction of this population of rocky planets orbits at sufficient distance that the climate may be suspected to be temperate in what is called the *habitable zone*. The understanding that this population of habitable Earth-like planets may be significant in size has pulled the question of extra-terrestrial life out of the realm of science-fiction. The desire to find such Earth-like exoplanets and signatures of extra-terrestrial life is strong, and will likely be the most compelling driver for exoplanet science for decades to come.

However to successfully answer the questions discussed here, astronomers must have the ability to understand in detail the planets that they observe. This thesis is focussed on observational and data analysis methods by which exoplanets can be characterized using their spectral properties.

1.1.2 *How to find exoplanets*

There are several ways to detect planets that orbit other stars. Three of these are relevant to the work described in this thesis, and these have incidentally also been the most successful in yielding exoplanet discoveries.

The most commonly used techniques rely on the indirect effect of the planet on the light that we observe from the system. The radial-velocity method (or Doppler method) makes use of the periodic motion of the star as it orbits around the center of mass of the planetary system, which is not in the exact center of the star. The varying radial velocity of the star causes a corresponding Doppler-shift of the stellar spectrum, which is monitored for multiple orbital periods in order to confirm the gravitational pull of a planet. Because this is a gravitational effect, the amplitude K of the radial-velocity variation of the star depends on the mass of the planet m_p, the mass of the star M_*, the eccentricity e and the orbital distance of the planet which is pro-

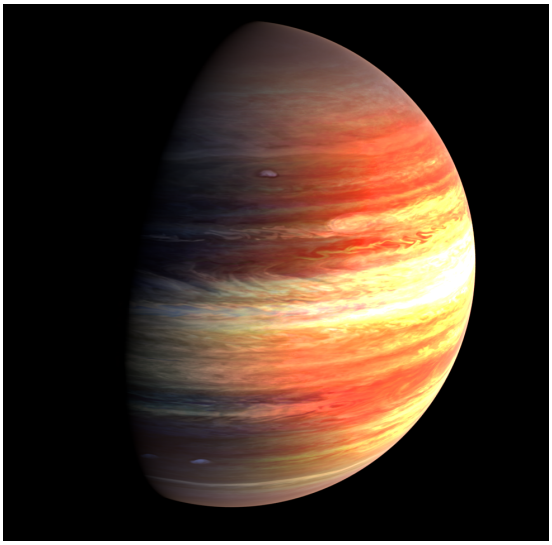

Figure 1.1: Artistic impression of what a hot Jupiter might look like.

portional to the orbital period P. This method is therefore mostly sensitive to massive planets in short-period orbits.

$$K = \left(\frac{2\pi G}{P}\right)^{\frac{1}{3}} \frac{m_p \sin(i)}{m_*^{\frac{2}{3}}} \frac{1}{\sqrt{1-e^2}}$$

The radial velocity method measures the velocity of the star along the line of sight. Velocity components in the plane perpendicular to the line of sight do not cause a Doppler effect, meaning that the radial velocity measurement also depends on the orientation of the orbital plane of the planet with respect to the line of sight. This orientation angle is quantified by the orbital inclination i. The magnitude of the radial velocity effect scales with $\sin i$, and the radial velocity method therefore yields only a lower limit to the mass of the planet.

The second method makes use of the fact that by chance, the orbital plane of some planets is aligned to our line-of-sight to the system (i.e. $i \sim 90°$). In this configuration, the planet passes in front of the stellar disk once during every orbit (see Figure 1.2). During such a transit, the planet blocks a fraction of the starlight, which can be detected in a photometric time-series of the system. The fraction of light blocked ($\frac{\Delta F}{F}$) is equal to the ratio of the projected areas of the disks of the planet and the star:

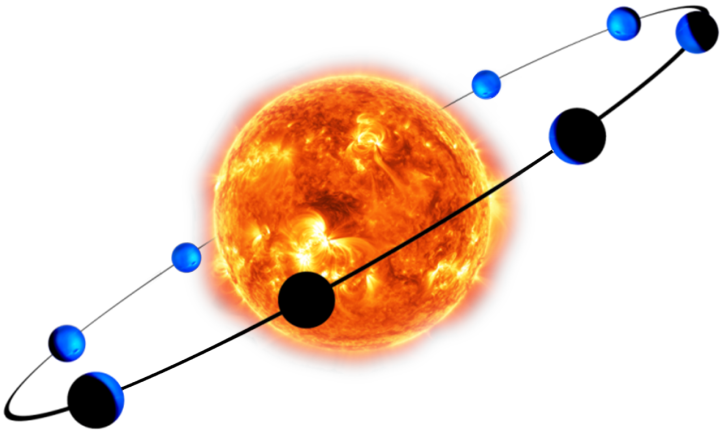

Figure 1.2: A planet in the transiting geometry. The transit occurs when the planet is in front of the star, while the secondary eclipse occurs when the planet moves behind it.

$$\frac{\Delta F}{F} = \frac{{R_p}^2}{{R_*}^2}$$

As such, this method is mostly sensitive to large planets in short orbits because a short orbital period allows for multiple transit events to be combined to increase the signal-to-noise. In addition, the likelihood of a favourable alignment is approximately proportional to the inverse of the orbital distance, which means that short-period planets are more likely to transit than planets further away from the star.

The transit of the planet also breaks the inclination degeneracy of the radial velocity method, allowing the true mass of the planet to be obtained. If the mass and radius of the star can be inferred independently, which is often the case, then the radial velocity and transit methods can be combined to reveal the mean density of the planet, which is a proxy for its composition and internal structure.

High-contrast imaging of an exoplanet system is the most direct way of finding exoplanets, but is often the most challenging. In high-contrast imaging, one tries to discern the point-source signal of the planet that is spatially separated from the much brighter host star. The wave-like nature of light fundamentally limits the spatial resolution of a telescope because it causes the light to diffract as it propagates through the aperture of the optical system. This diffraction pattern has a spatial extent that scales with wavelength and with the inverse of the size of the aperture. This means a point-source object is imaged as an extended Airy pattern on the detector, and that discerning

two closely separated point-sources is easiest for observations with large telescopes at short wavelengths.

In the case of a circular aperture, the diffraction pattern takes the form of an Airy function: A strong central peak surrounded by concentric rings that diminish away from the center. Two point source objects are considered to be resolved when their angular distance θ in radians is greater than $1.22\frac{\lambda}{D}$, where D is the diameter of the aperture.

However besides diffraction, ground-based telescopes are affected by distortion caused by the Earth's atmosphere that is highly variable in time. Visible to the naked eye, the *twinkling* of stars causes their image to be blurred, setting a limit to the angular resolution that can be achieved by ground-based telescopes (called the 'seeing' limit). Most planets are have an angular separation from their host star that is many times smaller than the seeing limit and are consequently masked by the distortion of the Earth's atmosphere. To counter this, ground-based high-contrast imaging instruments employ deformable optics (adaptive optics, AO) to correct for wave-front aberrations caused by atmospheric distortion in real-time (see e.g. Rousset et al., 2003; Beuzit et al., 2008; Jovanovic et al., 2015; Poyneer et al., 2016). High-quality AO systems can restore the image quality close to the diffraction limit, unlocking the full potential of large telescopes that would otherwise not be able to resolve spatial features smaller than the seeing limit.

Because high-contrast imaging works best for planets that are widely separated from their host stars, the sensitivity of this method is currently limited to a select part of the exoplanet population: Massive planets in wide orbits that are self-luminous due to the gradual release of primordial heat left-over from their formation. As such a system gets older, the contrast between the star and the planet increases and the planet becomes harder to observe directly. With current technology, high-contrast imaging is mostly limited to planets in orbits wider than ~ 5 AU in systems younger than ~ 1 Gyr (see e.g. Bowler, 2016). To be able to image cooler planets closer in requires the development of telescopes with large mirrors (needed to reduce the scale of the diffraction limit), combined with high-quality adaptive optics (often dubbed "extreme AO") and superior instrument stability.

1.1.3 *Unveiling the exoplanet population*

Over 25 years of exoplanet surveys have resulted in more than 3600 confirmed detections[2] (see Figure 1.3). Most of these planets were first discovered with the transit method. The most successful transit survey to date has been performed the Kepler Space Telescope, which has observed $\sim 150,000$ stars over a period of four years. It has identified over 4000 exoplanet candidates, of

2 Exoplanet.eu (Schneider et al., 2011)

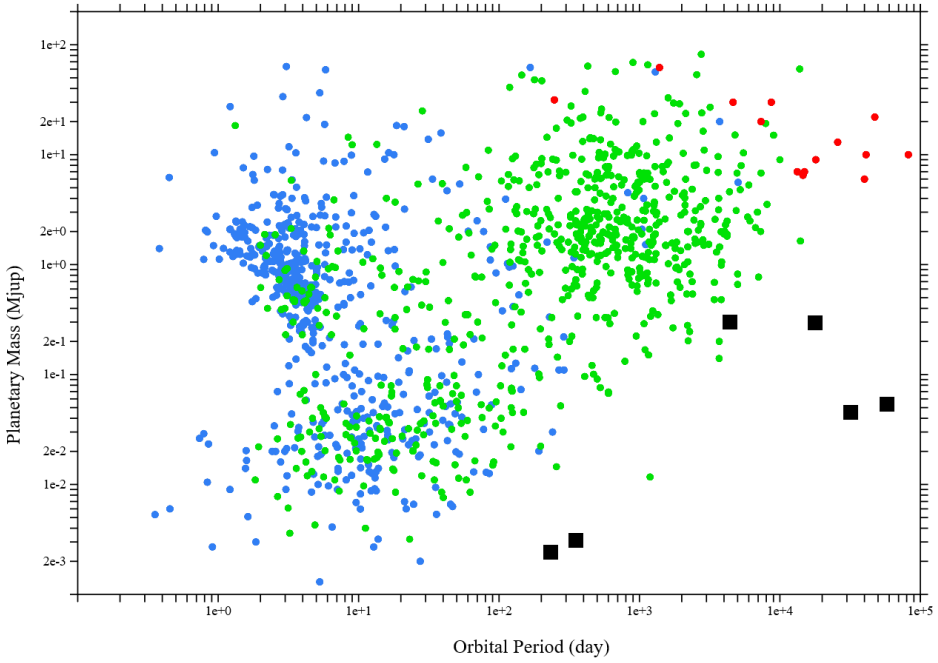

Figure 1.3: Confirmed exoplanet detections as of January 2017. Planets detected via radial velocity, transits an direct imaging are coloured green, blue and red respectively. The black squares indicate the solar system planets. Although the sensitivity of the planet-finding surveys generally decreases towards smaller planets at longer orbital periods, the detection of a large population of short-period rocky planets suggests that rocky planets far outnumber gas giants. Future planet-finding missions such as TESS and PLATO, as well as numerous ground-based transit and radial-velocity campaigns are predicted to better constrain the vast population of longer period rocky exoplanets.

which some 2300 have been independently confirmed[3]. Most of these planets reside in close orbits around their host stars with orbital periods of less than 20 days, and have radii greater than 2 Earth radii, which likely means that they have large gaseous envelopes (Howard et al., 2012; Owen et al., 2013; Fressin et al., 2013; Fulton et al., 2017). A fraction of these are comparable to the size of Jupiter, but most are smaller, and are referred to as warm Neptune analogues.

However, the high sensitivity of the Kepler light curves has also resulted in the discovery of ~ 1100 planets smaller than 2 Earth radii, which are likely to be rocky. This statistic indicates that there is a vast population of rocky

3 See https://www.nasa.gov/kepler/discoveries for the latest planet count.

planets straddling the inner regions of many, if not the majority of planetary systems (Petigura et al., 2013; Silburt et al., 2015; Burke et al., 2015; Mulders et al., 2016).

1.1.4 *Habitability*

A significant fraction of rocky exoplanets is expected to orbit their host stars in the *habitable zone*: at distances where the insolation is comparable to that of Earth so that the chemical environment at the planet surface could be favorable to life (Gaidos, 2013; Burke et al., 2015; Kane et al., 2016). There is no consensus about the extent of the habitable zone, because the amount of insolation that a planet receives is not the only determinant of habitability. The planet mass, size, composition and resulting atmospheric processes are also crucial factors (see e.g. Dole, 1964; Hart, 1979; Kopparapu et al., 2013; Zsom, 2015). The fact that habitability is the result of a complex interplay of processes is well illustrated by the planet Venus: Although similar to Earth in mass and composition and located on or near to the inner edge the habitable zone, the surface of Venus is one of the least hospitable places for life in the solar system because it attains an average surface temperature of 735 K due to the retention of sunlight and the resulting greenhouse effect. Furthermore, some rocky planets currently known are larger than the Earth and therefore significantly more massive. The solar system has no analogues of these *super-Earths*, which makes it even more difficult to predict the potential habitability of such planets.

For Sun-like stars, the habitable zone is roughly located between a distance of 0.5 to 2.5 AU from the Sun. Habitable planets in these systems therefore have orbital periods on the order of hundreds of days, limiting the sensitivity of photometric transit and radial velocity monitoring. This is why the search for habitable Earth-like planets is now focussed on M-dwarfs. Due to their low effective temperature, the habitable zone typically extends from 0.05 to 0.2 AU (Kopparapu, 2013) and therefore such planets have short periods in the order of 10 days. Recent high-profile discoveries of rocky planets around M-dwarfs include the detection of an $m \sin i = 1.3 m_E$ planet orbiting the nearby star Proxima Centauri b (Anglada-Escudé et al., 2016), and the discovery of seven transiting Earth-sized planets in the TRAPPIST-1 system (Gillon et al., 2016; Gillon et al., 2017), three of which are likely located in the habitable zone. Considering the size of the exoplanet population, ongoing and future planet-finding surveys will likely reveal a wealth of similar systems, each with potentially habitable planets.

However, the example of Venus above illustrates another important point: Venus's surface is perpetually covered by a thick cloud deck that hinders remote sensing of the surface below. Before the first radio observations pen-

etrated its dense atmosphere and revealed the extreme nature of the surface environment (Mayer et al., 1958), speculations about a temperate climate, the presence of molecular oxygen, water and even life on Venus were not uncommon (see e.g. Henkel, 1909; St. John et al., 1922; Whipple, 1931; Martz, 1934; Menzel et al., 1954). This demonstrates that planet climates are complex, and that a careful characterization of the atmospheres of Earth-like exoplanets is crucial to correctly assess their habitability.

1.2 SPECTROSCOPIC CHARACTERIZATION

1.2.1 *The spectrum of an exoplanet*

To learn more about a planet than its size and mass, the light of the planet must be studied directly. The spectral properties of the light that originates from the planet are determined by the thermal, chemical and material properties of its outer layers. The spectrum of an exoplanet is made up of two distinct components: Starlight that is reflected or scattered by the planet, and light that is emitted (thermally or otherwise) by the planet itself. Stars generally emit most of their radiation at optical wavelengths. The planet reflects a fraction of this light back into space, and the rest is absorbed and heats the atmosphere (Hansen, 2008). The fraction of all starlight that is not absorbed by the planet is called the *Bond Albedo*. Combined with any heat sources in the interior of the planet, the albedo determines the energy budget of the planet which in turn determines the overall temperature. To first order, the planet re-emits the absorbed starlight like a black-body, so the temperature of the planet can be constrained by measuring the amount of thermal radiation, possibly in multiple bands (see e.g. Charbonneau et al., 2005; Deming et al., 2006; Knutson et al., 2007; Harrington et al., 2007; Machalek et al., 2008; Gillon et al., 2010; Beaulieu et al., 2010; Smith et al., 2011; Demory et al., 2012; Demory et al., 2016).

The transiting geometry offers the possibility of *transmission* spectroscopy: Starlight that passes through the optically thin outer layers of the atmosphere is imprinted with absorption from the chemical constituents of the atmosphere (see e.g. Seager et al., 2000; Brown, 2001; Charbonneau et al., 2002; Tinetti et al., 2007; Barman, 2007; Burrows et al., 2008; Snellen et al., 2008; Désert et al., 2008; Sing et al., 2011). This effect manifests itself as a wavelength-dependence of the effective radius of the planet: At the wavelength of an atmospheric absorption line, the atmosphere is less transparent than at other wavelengths. This means that inside an absorption line, the planet causes a slightly deeper transit and will hence appear to be larger. The fractional increase of the apparent radius due to absorption by an atom or molecule in a layer ΔR above the effective radius R_p of the planet is:

$$\frac{2\Delta R\ R_p}{R_*^2}$$

ΔR is the height of the absorbing layer, and is generally proportional to the scale-height H of the atmosphere:

$$H = \frac{kT}{\mu g}$$

where T is the temperature, μ is the mean molecular weight and g is the surface gravity. This shows that some planets are more accessible to spectroscopic characterization than others, depending on the temperature, the atmospheric composition and the planet radius. This interpretation of the spectrum also indicates that the core of a spectral line represents a large value of ΔR, whereas the wings of the line correspond to smaller values of ΔR. Assuming that the opacity of the atmosphere decreases with altitude, this implies that the core of the line is formed high up in the atmosphere, whereas the wings of the line (in which the atom/molecule has an intrinsically smaller absorption cross-section) originate from deeper layers of the atmosphere. At the same time, the width of a spectral line depends on the local temperature and pressure. As such, the shape of an absorption line can in principle be used to constrain the thermal structure of the atmosphere (see e.g. Sing et al., 2008; Vidal-Madjar et al., 2011; Huitson et al., 2012; Schwarz et al., 2016).

Besides absorption by chemicals, another important source of opacity is scattering by aerosols and the blocking of light by optically thick clouds. Like on Earth, aerosols in the atmosphere tend to scatter radiation at short wavelengths, causing an apparent increase of the radius of a transiting exoplanet towards short wavelengths. The slope of the scattering spectrum can be be used to constrain the local temperature and molecular weight (Lecavelier Des Etangs et al., 2008; Benneke et al., 2012). Such observations have been performed on multiple occasions, mostly using the STIS and WFC3 on the Hubble Space Telescope which have coverage in the UV, optical and NIR. Transmission spectroscopy observations have also revealed that the spectra of many exoplanets are relatively featureless (e.g. Pont et al., 2008; Sing et al., 2009; Deming et al., 2013; Bento et al., 2014; Kreidberg et al., 2014; Nikolov et al., 2014; Sing et al., 2016; Kirk et al., 2017). The interpretation of these observations is that many planets possess cloud decks that make the atmosphere optically thick up to high altitudes, masking the layers that would otherwise produce absorption features.

Observations at infra-red wavelengths are sensitive to the thermally emitted radiation of the planet. This radiation traverses the upper optically thin layers of the atmosphere before being released into space, and may also carry imprints of the chemical species in the atmosphere (Seager et al., 2005;

Richardson et al., 2007). This radiation is most readily measured by observing the secondary eclipse of a transiting planet: Just before and after moving behind the star, the full day-side of the planet is in view. As the planet moves behind the star, this light is blocked, and the total amount of light observed from the system drops by an amount equal to the light emitted by the planet. Observing this difference at various wavelengths then reveals the thermal spectrum of the planet, constraining the dayside temperature and possible emission or absorption from atoms or molecules in the atmosphere. During the rest of the orbit, the observed flux of the system varies depending on what fraction of the day-side is in view, as well as the temperature difference between the day and night sides. Such *phase-curve* and secondary eclipse observations are regularly performed by the IRAC instrument aboard the Spitzer Space Telescope, which observes in two photometric bands at 3.6 μm and 4.5 μm, and until the depletion of its helium reservoir had access to bands at 5.3 μm and 8 μm. These observations have shown that hot Jupiters have strong day-to-night side temperature contrasts, hot-spots that are shifted away from the sub-stellar point by strong equatorial winds, and have even allowed day-side temperature maps to be derived (see e.g. Charbonneau et al., 2005; Deming et al., 2006; Deming et al., 2007; Demory et al., 2007; Charbonneau et al., 2008; Knutson et al., 2008; Gillon et al., 2010; Agol et al., 2010; Madhusudhan et al., 2011; Cowan et al., 2012; Demory et al., 2012; Todorov et al., 2013; Stevenson et al., 2014; Zellem et al., 2014; Demory et al., 2016).

Such observations have indicated that the hottest hot Jupiters may emit excess thermal light above what would be expected from their equilibrium temperature (Haynes et al., 2015; Evans et al., 2017). This has been explained by the presence of emission lines of water. Molecular lines are seen in emission when the layer in which the species is present is hotter than the layers below. This phenomenon is called a *thermal inversion layer*: an atmospheric layer in which the temperature increases with altitude. An inversion layer is caused by heating of the layer due to the presence of some chemical species that efficiently absorbs starlight. In the Earth's atmosphere, the ozone layer causes an inversion layer between altitudes of 10 km to 50 km, and similar processes are expected to occur in the atmospheres of hot Jupiters, albeit caused by different short-wavelength absorbers.

Titanium and vanadium oxide (TiO/VO) have rich optical absorption spectra that dominate the optical spectra of cool dwarf stars. Because the atmospheres of hot Jupiters can reach temperatures equivalent to the photospheres of the coolest stars, TiO and VO were naturally invoked as possible heat sources for inversion layers. The discovery of molecular emission at thermal wavelengths has therefore sparked searches for TiO and VO in transit transmission spectra, but until recently with very limited success (e.g. Désert et al., 2008; Evans et al., 2016).

1.2.2 *Spectral resolving power*

The difficulty in detecting molecular features in the spectra of exoplanets is partly because absorption bands of various molecules may overlap. If unknown quantities of molecular absorbers with overlapping absorption bands are mixed, the resulting absorption spectra can be difficult to interpret (Brogi et al., 2017). However, molecular absorption bands are composed of thousands to millions of individual absorption lines that are closely separated due to the fine structure of the energy levels of the molecule.

The resolving power R of a spectrograph describes the spectral scale $\Delta\lambda$ that can be resolved in a spectrum at wavelength λ:

$$R = \frac{\lambda}{\Delta\lambda}$$

The size and weight of a spectrograph generally increase proportionally with the amount of wavelength-dispersion because of the geometrical path-length required to convert a small dispersion angle to a large dispersion distance on the detector. This means that space-based spectrographs are typically limited to resolving powers of $R \sim 10^2$, at which the overall shape of the exoplanet spectrum can be resolved. In the optical, the spectrum is dominated by scattering by aerosols at blue wavelengths, strong atomic lines by alkali metals and the outlines of molecular absorption bands, but at $R \sim 10^2$, the latter cannot be resolved into individual absorption lines. However ground-based spectrographs can reach higher resolving powers of $R \sim 10^5$ at which individual spectral lines can be separated, allowing different molecular species to be distinguished at high confidence because the spectral fingerprint of each molecule is unique.

From the equation above, the resolving power can also be expressed in terms of the Doppler shift caused by a radial velocity Δv:

$$R = \frac{c}{\Delta v}$$

Current high-dispersion spectrographs can therefore resolve velocities down to a few $\mathrm{km\,s^{-1}}$. This is sufficient to resolve the orbital velocity of most planets, as well as the typical systematic velocity of the system relative to the Sun. This has the advantage that besides robust sensitivity to individual absorption lines, the planet can also be distinguished based on its velocity with respect to the host star and the Earth's atmosphere. High-dispersion observations therefore have the potential to strongly constrain the chemical composition of an exoplanet atmosphere.

1.2.3 *Cross-correlation*

The high dispersion of a high-resolution spectrograph means that the number of photons that is obtained per spectral element $\Delta\lambda$ is limited. For a typical high-dispersion transit observing sequence, the individual absorption lines are embedded in the photon noise of the much brighter star. Cross-correlation techniques can be used to match a model template spectrum to the observed spectrum to extract the planet spectrum from the noise. The cross-correlation $C(x, y)$ effectively measures the degree of similarity between a spectral template x_k and the noisy data y_k:

$$C(x, y) = \frac{\sum_{k=0}^{N}(x_k - \bar{x})(y_k - \bar{y})}{\sqrt{\sum_{k=0}^{N}(x_k - \bar{x})^2 \sum_{k=0}^{N-1}(y_k - \bar{y})^2}}$$

$C(x, y)$ varies between 1.0 (maximum correlation, i.e. when $y = ax + b$ with a and b constants and $a > 0$) and -1.0 (anti-correlation, i.e. when $a < 0$). The cross-correlation C is calculated for a range of radial velocity shifts of the template x. This yields the cross-correlation function $CCF(x, y, v)$, which measures the degree of overlap between the template and the data as a function of radial velocity v. The CCF peaks when the template is shifted to the same radial velocity as the data, and effectively co-adds all the absorption lines that are present in both the template and the data. This integration of the spectrum acts to average out the photon noise that is present at each spectral line, allowing the template spectrum to be detected even if the photon noise is stronger than the individual absorption lines.

The position of the cross-correlation peak in velocity space corresponds to the Doppler shift of the target spectrum at the time of the observations. As such, the CCF can be used to precisely measure the radial velocity of a target object. This technique has been used to detect molecular absorption by CO and H_2O in the day side emission spectra of a number of hot Jupiters (Snellen et al., 2010; Brogi et al., 2012; Brogi et al., 2013; Birkby et al., 2013; de Kok et al., 2013; Brogi et al., 2014; Lockwood et al., 2014; Brogi et al., 2016; Piskorz et al., 2016; Birkby et al., 2017; Piskorz et al., 2017). Also, it has enabled measurements of the instantaneous radial velocity of non-transiting hot Jupiters τ Bootis b, 51 Peg b and HD 179733 b yielding the orbital inclination i and therefore breaking the degeneracy with the planet mass that is inherent to the radial velocity method (Brogi et al., 2012; Brogi et al., 2013; Brogi et al., 2014). In addition, this technique has been used to measure the spin rate of hot giant planets β Pictoris b and GQ Lupi b, because the width of the cross-correlation function is partially due to velocity broadening caused by rotation of the planet (Snellen et al., 2014; Schwarz et al., 2016).

1.2.4 *Spectral dispersion and spatial resolution*

To increase the sensitivity of exoplanet observations, high-dispersion spectroscopy can be combined with high-contrast imaging (Sparks et al., 2002; Snellen et al., 2015). Light that originates from the planet is distinguished from the dominating starlight by simultaneously resolving the planet in the field, as well as using its spectral properties that are different from that of the star. This results in deeper contrast limits compared to traditional direct-imaging methods, especially close to the star where the signal of the planet is hard to distinguish from diffracted starlight (Lovis et al., 2017; Luger et al., 2017; Mawet et al., 2017; Wang et al., 2017).

To achieve this, the spectrograph needs to obtain spectra from a range of directions on the sky. One-dimensional spatial resolution can be achieved using a slit spectrograph: If the planet and the star are oriented parallel to the direction of the slit, the spatial separation between the two can be used to reject a fraction of the stellar spectrum if the planet and the star are resolved (Snellen et al., 2015). However, this requires knowledge about the orientation of the system, and spatial resolution is limited to one spatial dimension.

Integral-field spectrographs (IFS) achieve two-dimensional spatial resolution by dividing the field-of-view into separate sub-fields each of which is independently dispersed. This can be done using an image-slicer, which slices the field into multiple sub-slits (see Figure 1.4), or with an array of micro-lenses, each of which images a different part of the field of view. The data-reduction pipeline of an integral-field spectrograph typically produces a three-dimensional *data cube* from each science observation. Two axes of the cube represent the spatial dimensions on the sky, while the third dimension covers wavelength (see Figure 1.5). The addition of this third dimension of information means that a trade-off must be made between spatial and spectral resolution and coverage, because all the information needs to be contained on a two-dimensional detector. This trade-off is driven by the science-case for which the instrument is designed (see Chapter 3).

Integral-field spectrographs therefore have fewer detector pixels available for capturing spectral information compared to their high-dispersion counterparts. Both the VLT and Keck telescopes have near-infrared IFS's (SINFONI and OSIRIS) that can be operated in combination with their respective AO systems, making these instruments suitable for high-contrast imaging of hot young gas giants. The spectral resolving power lies in the range of $R \sim 3000$ to $R \sim 5000$, equivalent to radial velocities of 100 to 60 km s^{-1}. Such resolving power is not sufficient to resolve the orbital velocity of a planet or individual absorption lines, but the cross-correlation may still provide significant contrast enhancement (see Chapter 5).

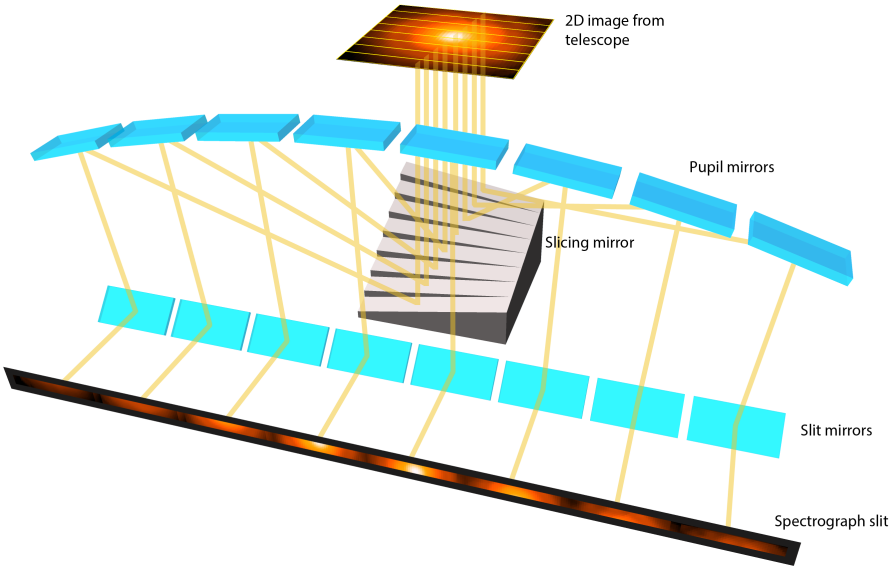

Figure 1.4: Conceptual representation of an image slicer used for integral-field slit-spectroscopy. The 2D image formed by the telescope is cut into a number of sub-slits which are re-imaged onto the entrance slit of the spectrograph side-by-side. These are then spectrally dispersed and imaged onto a two-dimensional CCD.

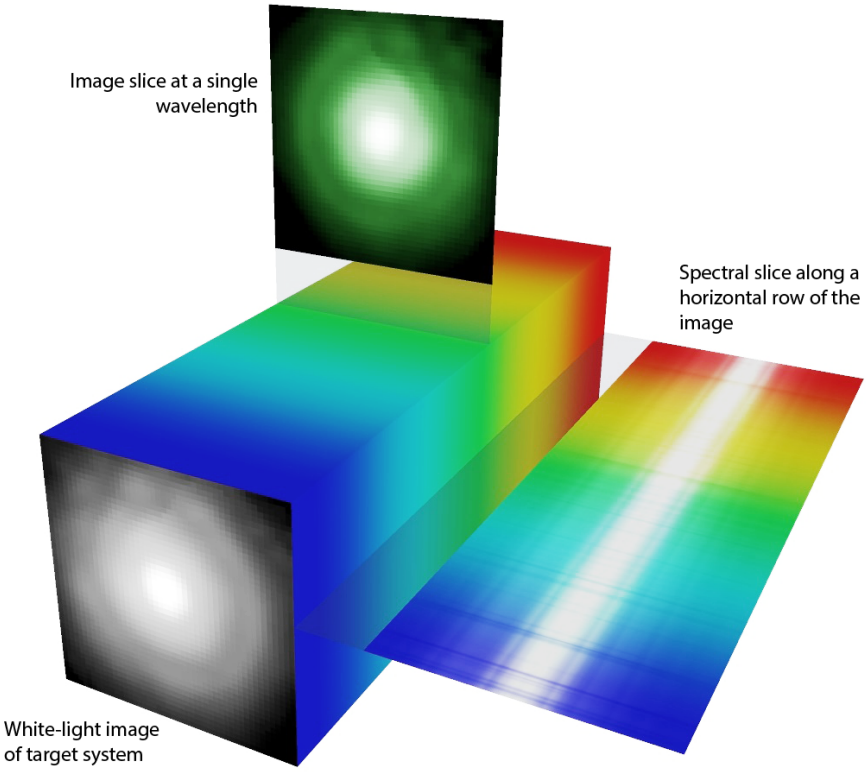

Figure 1.5: Graphical representation of a 3-dimensional data cube of an integral-field observation of an exoplanet system.

1.2.5 *Spectropolarimetry*

Light can be described as the propagation of a transversal wave in the electric and magnetic field according to the equations of Maxwell. The electric and magnetic fields oscillate in perpendicular planes and the spatial orientation of these planes together with the phase of the oscillation are referred to as the *polarization state* of light.

Thermal radiation is caused by the random motion of an ensemble of charged particles. Because of this random nature, thermal radiation has no preferred orientation on average, and the observed electric field vector oscillates randomly in all directions. Starlight is therefore *unpolarized*. However, this symmetry is broken upon reflection off a surface: Depending on the geometry and the properties of the medium, the wave that oscillates in the plane that is perpendicular to the surface of the medium will be attenuated. This means that starlight that is scattered by the atmosphere or surface of an exoplanet may be polarized by tens of percent, and this degree of polarization holds information about the scattering material. Polarization observations of exoplanets may therefore provide additional diagnostics of their atmospheres and surfaces (see e.g. Stam et al., 2004; Stam, 2008; Karalidi et al., 2012). In addition to preferentially selecting one polarization direction, some modes of scattering may also induce a phase delay between the polariation directions. This causes the field vector to rotate around the axis of propagation, and is referred to as circular polarization. Circular polarization occurs rarely in astronomical sources, and is mainly associated with complex organic molecules and biological processes (Sparks et al., 2009; Sparks et al., 2012).

Measurements of the polarization state of the exoplanet spectrum may unlock such observables in future observations of exoplanets. However, these observations will be challenging because absolute calibration of polarization measurements is technologically difficult and because the global appearance of such biomarkers on exoplanets are not yet experimentally corroborated (see Chapter 3).

1.3 THIS THESIS

If astronomers want to fully understand and characterize exoplanets, astronomical observations must overcome extreme contrasts and reliably measure the intensity and polarization over large ranges of the electromagnetic spectrum at high spectral and spatial resolving power. The work presented in this thesis aims to contribute to this endeavour by applying and developing new ways to perform and analyse exoplanet observations. As larger, more sensitive facilities are being developed, these techniques may be used in the

future to characterize the surface environments of exoplanets, to assess their habitability and potentially to aid in the discovery of extra-terrestrial life.

Chapter 2 describes the application of the cross-correlation method to search for gaseous TiO in the atmosphere of hot Jupiter HD 209458 b, potentially associated with a thermal inversion layer. The data was obtained by the high-dispersion spectrograph (HDS) on the Subaru telescope, and spans one transit of HD 209458 b at optical wavelengths. The TiO molecule has millions of absorption lines throughout the optical. We find that this dataset can be used to discern the presence of TiO in the atmosphere in HD 209458 b down to volume mixing ratios below 10^{-9}. However, the theoretical line-lists that are used to model the template spectrum needed to cross-correlate the data with, are inaccurate at high spectral resolution, hampering application of cross-correlation. This paper therefore advocates for more precise modelling of the energy levels of TiO and other relevant molecules, or spectroscopic measurements in the laboratory. This work has previously appeared in A&A (Hoeijmakers et al., 2015).

Chapter 3 presents a prototype for the Lunar Observatory for Unresolved Polarimetry of Earth (LOUPE). This instrument is designed to observe the Earth from the surface of the Moon and characterize its optical linear polarization spectrum as if it was an exoplanet. These data are needed to benchmark future polarization observations of potentially habitable exoplanets. We show that such an instrument can be small, robust and fully solid-state, which is essential for application and reliable operation in space. This work has been published in Optics Express (Hoeijmakers et al., 2016).

Chapter 4 presents an analysis of over 2000 archival high-resolution optical spectra of the τ Boötis system to search for the reflected light of the non-transiting hot Jupiter τ Boötis b. This data was obtained by various spectrographs between 1998 and 2011, and when combined provides a 1σ sensitivity to the reflected stellar spectrum of 5.0×10^{-6} times the brightness of the star. The planet is not detected however, which means that it likely has an albedo $p < 0.11$. Although low, such albedo values are not uncommon for hot Jupiters as evidenced by phase-curve observations by space telescopes.

Chapter 5 presents the first application of the cross-correlation technique to high-contrast imaging observations of the young gas giant β Pictoris b, obtained by the SINFONI integral-field spectrograph at the VLT in K-band. We successfully remove the stellar flux from the data and reveal the planet by cross-correlating with model spectra of CO and H_2O. The

cross-correlation function produces *molecule maps* of the system, which provide an alternative to established high-contrast imaging methods that suffer from residual starlight, especially at small angular distances from the star. We show that this technique has significant potential when applied with data of NIRSpec, MIRI and HARMONI; upcoming medium-resolution integral-field spectrographs on the James Webb Space Telescope and the ELT.

BIBLIOGRAPHY

Agol, E. et al. (2010). „The Climate of HD 189733b from Fourteen Transits and Eclipses Measured by Spitzer." In: *ApJ* 721, pp. 1861–1877. DOI: 10.1088/0004-637X/721/2/1861. arXiv: 1007.4378 [astro-ph.EP].

Anglada-Escudé, G. et al. (2016). „A terrestrial planet candidate in a temperate orbit around Proxima Centauri." In: *Nature* 536, pp. 437–440. DOI: 10.1038/nature19106. arXiv: 1609.03449 [astro-ph.EP].

Barman, T. (2007). „Identification of Absorption Features in an Extrasolar Planet Atmosphere." In: *ApJ* 661, pp. L191–L194. DOI: 10.1086/518736. arXiv: 0704.1114.

Beaulieu, J. P. et al. (2010). „Water in the atmosphere of HD 209458b from 3.6-8 μm IRAC photometric observations in primary transit." In: *MNRAS* 409, pp. 963–974. DOI: 10.1111/j.1365-2966.2010.16516.x. arXiv: 0909.0185 [astro-ph.EP].

Benneke, B. and S. Seager (2012). „Atmospheric Retrieval for Super-Earths: Uniquely Constraining the Atmospheric Composition with Transmission Spectroscopy." In: *ApJ* 753, 100, p. 100. DOI: 10.1088/0004-637X/753/2/100. arXiv: 1203.4018 [astro-ph.EP].

Bento, J. et al. (2014). „Optical transmission photometry of the highly inflated exoplanet WASP-17b." In: *MNRAS* 437, pp. 1511–1518. DOI: 10.1093/mnras/stt1979. arXiv: 1310.3893 [astro-ph.EP].

Beuzit, J.-L. et al. (2008). „SPHERE: a 'Planet Finder' instrument for the VLT." In: *Ground-based and Airborne Instrumentation for Astronomy II*. Vol. 7014. Proc. SPIE, p. 701418. DOI: 10.1117/12.790120.

Birkby, J. L. et al. (2013). „Detection of water absorption in the day side atmosphere of HD 189733 b using ground-based high-resolution spectroscopy at 3.2 μm." In: *MNRAS* 436, pp. L35–L39. DOI: 10.1093/mnrasl/slt107. arXiv: 1307.1133 [astro-ph.EP].

Birkby, J. L. et al. (2017). „Discovery of Water at High Spectral Resolution in the Atmosphere of 51 Peg b." In: *AJ* 153, 138, p. 138. DOI: 10.3847/1538-3881/aa5c87. arXiv: 1701.07257 [astro-ph.EP].

Boss, A. P. (1997). „Giant planet formation by gravitational instability." In: *Science* 276, pp. 1836–1839. DOI: 10.1126/science.276.5320.1836.

Bowler, B. P. (2016). „Imaging Extrasolar Giant Planets." In: *PASP* 128.10, p. 102001. DOI: 10.1088/1538-3873/128/968/102001. arXiv: 1605.02731 [astro-ph.EP].

Brogi, M. et al. (2012). „The signature of orbital motion from the dayside of the planet τ Boötis b." In: *Nature* 486, pp. 502–504. DOI: 10.1038/nature11161. arXiv: 1206.6109 [astro-ph.EP].

Brogi, M. et al. (2013). „Detection of Molecular Absorption in the Dayside of Exoplanet 51 Pegasi b?" In: *ApJ* 767, 27, p. 27. DOI: 10.1088/0004-637X/767/1/27. arXiv: 1302.6242 [astro-ph.EP].

Brogi, M. et al. (2014). „Carbon monoxide and water vapor in the atmosphere of the non-transiting exoplanet HD 179949 b." In: *A&A* 565, A124, A124. DOI: 10.1051/0004-6361/201423537. arXiv: 1404.3769 [astro-ph.EP].

Brogi, M. et al. (2016). „Rotation and Winds of Exoplanet HD 189733 b Measured with High-dispersion Transmission Spectroscopy." In: *ApJ* 817, 106, p. 106. DOI: 10.3847/0004-637X/817/2/106. arXiv: 1512.05175 [astro-ph.EP].

Brogi, M. et al. (2017). „A Framework to Combine Low- and High-resolution Spectroscopy for the Atmospheres of Transiting Exoplanets." In: *ApJ* 839, L2, p. L2. DOI: 10.3847/2041-8213/aa6933. arXiv: 1612.07008 [astro-ph.EP].

Brown, T. M. (2001). „Transmission Spectra as Diagnostics of Extrasolar Giant Planet Atmospheres." In: *ApJ* 553, pp. 1006–1026. DOI: 10.1086/320950. eprint: astro-ph/0101307.

Burke, C. J. et al. (2015). „Terrestrial Planet Occurrence Rates for the Kepler GK Dwarf Sample." In: *ApJ* 809, 8, p. 8. DOI: 10.1088/0004-637X/809/1/8. arXiv: 1506.04175 [astro-ph.EP].

Burrows, A., J. Budaj, and I. Hubeny (2008). „Theoretical Spectra and Light Curves of Close-in Extrasolar Giant Planets and Comparison with Data." In: *ApJ* 678, 1436-1457, pp. 1436–1457. DOI: 10.1086/533518. arXiv: 0709.4080.

Butler, R. P. et al. (2006). „Catalog of Nearby Exoplanets." In: *ApJ* 646, pp. 505–522. DOI: 10.1086/504701. eprint: astro-ph/0607493.

Charbonneau, D. et al. (2002). „Detection of an Extrasolar Planet Atmosphere." In: *ApJ* 568, pp. 377–384. DOI: 10.1086/338770. eprint: astro-ph/0111544.

Charbonneau, D. et al. (2005). „Detection of Thermal Emission from an Extrasolar Planet." In: *ApJ* 626, pp. 523–529. DOI: 10.1086/429991. eprint: astro-ph/0503457.

Charbonneau, D. et al. (2008). „The Broadband Infrared Emission Spectrum of the Exoplanet HD 189733b." In: *ApJ* 686, 1341-1348, pp. 1341–1348. DOI: 10.1086/591635. arXiv: 0802.0845.

Coughlin, J. L. et al. (2016). „Planetary Candidates Observed by Kepler. VII. The First Fully Uniform Catalog Based on the Entire 48-month Data Set (Q1-Q17 DR24)." In: *ApJ* 224, 12, p. 12. DOI: 10.3847/0067-0049/224/1/12. arXiv: 1512.06149 [astro-ph.EP].

Cowan, N. B. et al. (2012). „Thermal Phase Variations of WASP-12b: Defying Predictions." In: *ApJ* 747, 82, p. 82. DOI: 10.1088/0004-637X/747/1/82. arXiv: 1112.0574 [astro-ph.EP].

de Kok, R. J. et al. (2013). „Detection of carbon monoxide in the high-resolution day-side spectrum of the exoplanet HD 189733b." In: *A&A* 554, A82, A82. DOI: 10.1051/0004-6361/201321381. arXiv: 1304.4014 [astro-ph.EP].

Deming, D. et al. (2006). „Strong Infrared Emission from the Extrasolar Planet HD 189733b." In: *ApJ* 644, pp. 560–564. DOI: 10.1086/503358. eprint: astro-ph/0602443.

Deming, D. et al. (2007). „Spitzer Transit and Secondary Eclipse Photometry of GJ 436b." In: *ApJ* 667, pp. L199–L202. DOI: 10.1086/522496. arXiv: 0707.2778.

Deming, D. et al. (2013). „Infrared Transmission Spectroscopy of the Exoplanets HD 209458b and XO-1b Using the Wide Field Camera-3 on the Hubble Space Telescope." In: *ApJ* 774, 95, p. 95. DOI: 10.1088/0004-637X/774/2/95. arXiv: 1302.1141 [astro-ph.EP].

Demory, B.-O. et al. (2007). „Characterization of the hot Neptune GJ 436 b with Spitzer and ground-based observations." In: *A&A* 475, pp. 1125–1129. DOI: 10.1051/0004-6361:20078354. arXiv: 0707.3809.

Demory, B.-O. et al. (2012). „Detection of Thermal Emission from a Super-Earth." In: *ApJ* 751, L28, p. L28. DOI: 10.1088/2041-8205/751/2/L28. arXiv: 1205.1766 [astro-ph.EP].

Demory, B.-O. et al. (2016). „A map of the large day-night temperature gradient of a super-Earth exoplanet." In: *Nature* 532, pp. 207–209. DOI: 10.1038/nature17169. arXiv: 1604.05725 [astro-ph.EP].

Désert, J.-M. et al. (2008). „TiO and VO broad band absorption features in the optical spectrum of the atmosphere of the hot-Jupiter HD 209458b." In: *A&A* 492, pp. 585–592. DOI: 10.1051/0004-6361:200810355. arXiv: 0809.1865.

Dole, S. H. (1964). *Habitable planets for man*.

Evans, T. M. et al. (2016). „Detection of H_2O and Evidence for TiO/VO in an Ultra-hot Exoplanet Atmosphere." In: *ApJ* 822, L4, p. L4. DOI: 10.3847/2041-8205/822/1/L4. arXiv: 1604.02310 [astro-ph.EP].

Evans, T. M. et al. (2017). „An ultrahot gas-giant exoplanet with a stratosphere." In: *Nature* 548, pp. 58–61. DOI: 10.1038/nature23266. arXiv: 1708.01076 [astro-ph.EP].

Foreman-Mackey, D., D. W. Hogg, and T. D. Morton (2014). „Exoplanet Population Inference and the Abundance of Earth Analogs from Noisy, Incomplete Catalogs." In: *ApJ* 795, 64, p. 64. DOI: 10.1088/0004-637X/795/1/64. arXiv: 1406.3020 [astro-ph.EP].

Fressin, F. et al. (2013). „The False Positive Rate of Kepler and the Occurrence of Planets." In: *ApJ* 766, 81, p. 81. DOI: 10.1088/0004-637X/766/2/81. arXiv: 1301.0842 [astro-ph.EP].

Fulton, B. J. et al. (2017). „The California-Kepler Survey. III. A Gap in the Radius Distribution of Small Planets." In: *ArXiv e-prints*. arXiv: 1703.10375 [astro-ph.EP].

Gaidos, E. (2013). „Candidate Planets in the Habitable Zones of Kepler Stars." In: *ApJ* 770, 90, p. 90. DOI: 10.1088/0004-637X/770/2/90. arXiv: 1301.2384 [astro-ph.EP].

Gillon, M. et al. (2010). „The thermal emission of the young and massive planet CoRoT-2b at 4.5 and 8 μm." In: *A&A* 511, A3, A3. DOI: 10.1051/0004-6361/200913507. arXiv: 0911.5087 [astro-ph.EP].

Gillon, M. et al. (2016). „Temperate Earth-sized planets transiting a nearby ultracool dwarf star." In: *Nature* 533, pp. 221–224. DOI: 10.1038/nature17448. arXiv: 1605.07211 [astro-ph.EP].

Gillon, M. et al. (2017). „Seven temperate terrestrial planets around the nearby ultracool dwarf star TRAPPIST-1." In: *Nature* 542, pp. 456–460. DOI: 10.1038/nature21360. arXiv: 1703.01424 [astro-ph.EP].

Gomes, R. et al. (2005). „Origin of the cataclysmic Late Heavy Bombardment period of the terrestrial planets." In: *Nature* 435, pp. 466–469. DOI: 10.1038/nature03676.

Hansen, B. M. S. (2008). „On the Absorption and Redistribution of Energy in Irradiated Planets." In: *ApJ* 179, 484-508, pp. 484–508. DOI: 10.1086/591964. arXiv: 0801.2972.

Hansen, B. M. S., H.-Y. Shih, and T. Currie (2009). „The Pulsar Planets: A Test Case of Terrestrial Planet Assembly." In: *ApJ* 691, pp. 382–393. DOI: 10.1088/0004-637X/691/1/382. arXiv: 0908.0736 [astro-ph.EP].

Harrington, J. et al. (2007). „The hottest planet." In: *Nature* 447, pp. 691–693. DOI: 10.1038/nature05863.

Hart, M. H. (1979). „Habitable Zones about Main Sequence Stars." In: *Icarus* 37, pp. 351–357. DOI: 10.1016/0019-1035(79)90141-6.

Haynes, K. et al. (2015). „Spectroscopic Evidence for a Temperature Inversion in the Dayside Atmosphere of Hot Jupiter WASP-33b." In: *ApJ* 806, 146, p. 146. DOI: 10.1088/0004-637X/806/2/146. arXiv: 1505.01490 [astro-ph.EP].

Henkel, F. W. (1909). „Venus as the Abode of Life." In: *Popular Astronomy* 17, pp. 412–417.

Hennebelle, P. and G. Chabrier (2008). „Analytical Theory for the Initial Mass Function: CO Clumps and Prestellar Cores." In: *ApJ* 684, 395-410, pp. 395–410. DOI: 10.1086/589916. arXiv: 0805.0691.

Hoeijmakers, H. J. et al. (2015). „A search for TiO in the optical high-resolution transmission spectrum of HD 209458b: Hindrance due to inaccuracies in the line database." In: *A&A* 575, A20, A20. DOI: 10.1051/0004-6361/201424794. arXiv: 1411.6017 [astro-ph.EP].

Hoeijmakers, H. J. et al. (2016). „Design trade-off and proof of concept for LOUPE, the Lunar Observatory for Unresolved Polarimetry of Earth." In: *Optics Express* 24, p. 21435. DOI: 10.1364/OE.24.021435.

Howard, A. W. et al. (2012). „Planet Occurrence within 0.25 AU of Solar-type Stars from Kepler." In: *ApJ* 201, 15, p. 15. DOI: 10.1088/0067-0049/201/2/15. arXiv: 1103.2541 [astro-ph.EP].

Huitson, C. M. et al. (2012). „Temperature-pressure profile of the hot Jupiter HD 189733b from HST sodium observations: detection of upper atmo-

spheric heating." In: *MNRAS* 422, pp. 2477–2488. DOI: 10.1111/j.1365-2966.2012.20805.x. arXiv: 1202.4721 [astro-ph.EP].

Ida, S., J. Larwood, and A. Burkert (2000). „Evidence for Early Stellar Encounters in the Orbital Distribution of Edgeworth-Kuiper Belt Objects." In: *ApJ* 528, pp. 351–356. DOI: 10.1086/308179. eprint: astro-ph/9907217.

Jovanovic, N. et al. (2015). „The Subaru Coronagraphic Extreme Adaptive Optics System: Enabling High-Contrast Imaging on Solar-System Scales." In: *PASP* 127, p. 890. DOI: 10.1086/682989. arXiv: 1507.00017 [astro-ph.IM].

Kane, S. R. et al. (2016). „A Catalog of Kepler Habitable Zone Exoplanet Candidates." In: *ApJ* 830, 1, p. 1. DOI: 10.3847/0004-637X/830/1/1. arXiv: 1608.00620 [astro-ph.EP].

Karalidi, T. and D. M. Stam (2012). „Modeled flux and polarization signals of horizontally inhomogeneous exoplanets applied to Earth-like planets." In: *A&A* 546, A56, A56. DOI: 10.1051/0004-6361/201219297. arXiv: 1210.3198 [astro-ph.EP].

Kerr, M. et al. (2015). „Limits on Planet Formation Around Young Pulsars and Implications for Supernova Fallback Disks." In: *ApJ* 809, L11, p. L11. DOI: 10.1088/2041-8205/809/1/L11. arXiv: 1507.06982 [astro-ph.HE].

Kirk, J. et al. (2017). „Rayleigh scattering in the transmission spectrum of HAT-P-18b." In: *MNRAS* 468, pp. 3907–3916. DOI: 10.1093/mnras/stx752. arXiv: 1611.06916 [astro-ph.EP].

Knutson, H. A. et al. (2007). „A map of the day-night contrast of the extrasolar planet HD 189733b." In: *Nature* 447, pp. 183–186. DOI: 10.1038/nature05782. arXiv: 0705.0993.

Knutson, H. A. et al. (2008). „The 3.6-8.0 μm Broadband Emission Spectrum of HD 209458b: Evidence for an Atmospheric Temperature Inversion." In: *ApJ* 673, 526-531, pp. 526–531. DOI: 10.1086/523894. arXiv: 0709.3984.

Kopparapu, R. K. (2013). „A Revised Estimate of the Occurrence Rate of Terrestrial Planets in the Habitable Zones around Kepler M-dwarfs." In: *ApJ* 767, L8, p. L8. DOI: 10.1088/2041-8205/767/1/L8. arXiv: 1303.2649 [astro-ph.EP].

Kopparapu, R. K. et al. (2013). „Habitable Zones around Main-sequence Stars: New Estimates." In: *ApJ* 765, 131, p. 131. DOI: 10.1088/0004-637X/765/2/131. arXiv: 1301.6674 [astro-ph.EP].

Kreidberg, L. et al. (2014). „Clouds in the atmosphere of the super-Earth exoplanet GJ1214b." In: *Nature* 505, pp. 69–72. DOI: 10.1038/nature12888. arXiv: 1401.0022 [astro-ph.EP].

Laughlin, G. and F. C. Adams (1998). „The Modification of Planetary Orbits in Dense Open Clusters." In: *ApJ* 508, pp. L171–L174. DOI: 10.1086/311736.

Lecavelier Des Etangs, A. et al. (2008). „Rayleigh scattering by H_2 in the extrasolar planet HD 209458b." In: *A&A* 485, pp. 865–869. DOI: 10.1051/0004-6361:200809704. arXiv: 0805.0595.

Levison, H. F. et al. (2008). „Origin of the structure of the Kuiper belt during a dynamical instability in the orbits of Uranus and Neptune." In: *Icarus* 196, pp. 258–273. DOI: 10.1016/j.icarus.2007.11.035. arXiv: 0712.0553.

Lockwood, A. C. et al. (2014). „Near-IR Direct Detection of Water Vapor in Tau Boötis b." In: *ApJ* 783, L29, p. L29. DOI: 10.1088/2041-8205/783/2/L29. arXiv: 1402.0846 [astro-ph.EP].

Lovis, C. et al. (2017). „Atmospheric characterization of Proxima b by coupling the SPHERE high-contrast imager to the ESPRESSO spectrograph." In: *A&A* 599, A16, A16. DOI: 10.1051/0004-6361/201629682. arXiv: 1609.03082 [astro-ph.EP].

Luger, R. et al. (2017). „The Pale Green Dot: A Method to Characterize Proxima Centauri b Using Exo-Aurorae." In: *ApJ* 837, 63, p. 63. DOI: 10.3847/1538-4357/aa6040. arXiv: 1609.09075 [astro-ph.EP].

Machalek, P. et al. (2008). „Thermal Emission of Exoplanet XO-1b." In: *ApJ* 684, 1427-1432, pp. 1427–1432. DOI: 10.1086/590140. arXiv: 0805.2418.

Madhusudhan, N., M. A. Amin, and G. M. Kennedy (2014). „Toward Chemical Constraints on Hot Jupiter Migration." In: *ApJ* 794, L12, p. L12. DOI: 10.1088/2041-8205/794/1/L12. arXiv: 1408.3668 [astro-ph.EP].

Madhusudhan, N. et al. (2011). „A high C/O ratio and weak thermal inversion in the atmosphere of exoplanet WASP-12b." In: *Nature* 469, pp. 64–67. DOI: 10.1038/nature09602. arXiv: 1012.1603 [astro-ph.EP].

Martz Jr., E. P. (1934). „Venus and life." In: *Popular Astronomy* 42, p. 165.

Mawet, D. et al. (2017). „Observing Exoplanets with High-dispersion Coronagraphy. II. Demonstration of an Active Single-mode Fiber Injection Unit." In: *ApJ* 838, 92, p. 92. DOI: 10.3847/1538-4357/aa647f. arXiv: 1703.00583 [astro-ph.EP].

Mayer, C. H., T. P. McCullough, and R. M. Sloanaker (1958). „Observations of Venus at 3.15-CM Wave Length." In: *ApJ* 127, p. 1. DOI: 10.1086/146433.

Mayor, M. and D. Queloz (1995). „A Jupiter-mass companion to a solar-type star." In: *Nature* 378, pp. 355–359. DOI: 10.1038/378355a0.

Menzel, D. H. and F. L. Whipple (1954). „The case for H2O clouds on Venus." In: *AJ* 59, p. 329. DOI: 10.1086/107037.

Miller, M. C. and D. P. Hamilton (2001). „Implications of the PSR 1257+12 Planetary System for Isolated Millisecond Pulsars." In: *ApJ* 550, pp. 863–870. DOI: 10.1086/319813. eprint: astro-ph/0012042.

Mulders, G. D. et al. (2016). „A Super-solar Metallicity for Stars with Hot Rocky Exoplanets." In: *AJ* 152, 187, p. 187. DOI: 10.3847/0004-6256/152/6/187. arXiv: 1609.05898 [astro-ph.EP].

Nikolov, N. et al. (2014). „Hubble Space Telescope hot Jupiter transmission spectral survey: a detection of Na and strong optical absorption in HAT-P-1b." In: *MNRAS* 437, pp. 46–66. DOI: 10.1093/mnras/stt1859. arXiv: 1310.0083 [astro-ph.SR].

Öberg, K. I., R. Murray-Clay, and E. A. Bergin (2011). „The Effects of Snowlines on C/O in Planetary Atmospheres." In: *ApJ* 743, L16, p. L16. DOI: 10.1088/2041-8205/743/1/L16. arXiv: 1110.5567.

Owen, J. E. and Y. Wu (2013). „Kepler Planets: A Tale of Evaporation." In: *ApJ* 775, 105, p. 105. DOI: 10.1088/0004-637X/775/2/105. arXiv: 1303.3899 [astro-ph.EP].

Petigura, E. A., A. W. Howard, and G. W. Marcy (2013). „Prevalence of Earth-size planets orbiting Sun-like stars." In: *Proceedings of the National Academy of Science* 110, pp. 19273–19278. DOI: 10.1073/pnas.1319909110. arXiv: 1311.6806 [astro-ph.EP].

Piskorz, D. et al. (2016). „Evidence for the Direct Detection of the Thermal Spectrum of the Non-Transiting Hot Gas Giant HD 88133 b." In: *ApJ* 832, 131, p. 131. DOI: 10.3847/0004-637X/832/2/131. arXiv: 1609.09074 [astro-ph.EP].

Piskorz, D. et al. (2017). „Detection of Water Vapor in the Thermal Spectrum of the Non-transiting Hot Jupiter Upsilon Andromedae b." In: *AJ* 154, 78, p. 78. DOI: 10.3847/1538-3881/aa7dd8. arXiv: 1707.01534 [astro-ph.EP].

Pollack, J. B. et al. (1996). „Formation of the Giant Planets by Concurrent Accretion of Solids and Gas." In: *Icarus* 124, pp. 62–85. DOI: 10.1006/icar.1996.0190.

Pont, F. et al. (2008). „Detection of atmospheric haze on an extrasolar planet: the 0.55-1.05 μm transmission spectrum of HD 189733b with the HubbleSpaceTelescope." In: *MNRAS* 385, pp. 109–118. DOI: 10.1111/j.1365-2966.2008.12852.x. arXiv: 0712.1374.

Poyneer, L. A. et al. (2016). „Performance of the Gemini Planet Imager's adaptive optics system." In: *Ap. Opt.* 55, p. 323. DOI: 10.1364/AO.55.000323.

Rasio, F. A. and E. B. Ford (1996). „Dynamical instabilities and the formation of extrasolar planetary systems." In: *Science* 274, pp. 954–956. DOI: 10.1126/science.274.5289.954.

Richardson, L. J. et al. (2007). „A spectrum of an extrasolar planet." In: *Nature* 445, pp. 892–895. DOI: 10.1038/nature05636. eprint: astro-ph/0702507.

Rousset, G. et al. (2003). „NAOS, the first AO system of the VLT: on-sky performance." In: *Adaptive Optical System Technologies II*. Ed. by P. L. Wizinowich and D. Bonaccini. Vol. 4839. Proc. SPIE, pp. 140–149. DOI: 10.1117/12.459332.

Schneider, J. et al. (2011). „Defining and cataloging exoplanets: the exoplanet.eu database." In: *A&A* 532, A79, A79. DOI: 10.1051/0004-6361/201116713. arXiv: 1106.0586 [astro-ph.EP].

Schwarz, H. et al. (2016). „The slow spin of the young substellar companion GQ Lupi b and its orbital configuration." In: *A&A* 593, A74, A74. DOI: 10.1051/0004-6361/201628908. arXiv: 1607.00012 [astro-ph.EP].

Seager, S. and D. D. Sasselov (2000). „Theoretical Transmission Spectra during Extrasolar Giant Planet Transits." In: *ApJ* 537, pp. 916–921. DOI: 10.1086/309088. eprint: astro-ph/9912241.

Seager, S. et al. (2005). „On the Dayside Thermal Emission of Hot Jupiters." In: *ApJ* 632, pp. 1122–1131. DOI: 10.1086/444411. eprint: astro-ph/0504212.

Silburt, A., E. Gaidos, and Y. Wu (2015). „A Statistical Reconstruction of the Planet Population around Kepler Solar-type Stars." In: *ApJ* 799, 180, p. 180. DOI: 10.1088/0004-637X/799/2/180. arXiv: 1406.6048 [astro-ph.EP].

Sing, D. K. et al. (2008). „Determining Atmospheric Conditions at the Terminator of the Hot Jupiter HD 209458b." In: *ApJ* 686, 667-673, pp. 667–673. DOI: 10.1086/590076. arXiv: 0803.1054.

Sing, D. K. et al. (2009). „Transit spectrophotometry of the exoplanet HD 189733b. I. Searching for water but finding haze with HST NICMOS." In: *A&A* 505, pp. 891–899. DOI: 10.1051/0004-6361/200912776. arXiv: 0907.4991 [astro-ph.EP].

Sing, D. K. et al. (2011). „Gran Telescopio Canarias OSIRIS transiting exoplanet atmospheric survey: detection of potassium in XO-2b from narrowband spectrophotometry." In: *A&A* 527, A73, A73. DOI: 10.1051/0004-6361/201015579. arXiv: 1008.4795 [astro-ph.EP].

Sing, D. K. et al. (2016). „A continuum from clear to cloudy hot-Jupiter exoplanets without primordial water depletion." In: *Nature* 529, pp. 59–62. DOI: 10.1038/nature16068. arXiv: 1512.04341 [astro-ph.EP].

Smith, A. M. S. et al. (2011). „Thermal emission from WASP-33b, the hottest known planet." In: *MNRAS* 416, pp. 2096–2101. DOI: 10.1111/j.1365-2966.2011.19187.x. arXiv: 1101.2432 [astro-ph.EP].

Snellen, I. A. G. et al. (2008). „Ground-based detection of sodium in the transmission spectrum of exoplanet HD 209458b." In: *A&A* 487, pp. 357–362. DOI: 10.1051/0004-6361:200809762. arXiv: 0805.0789.

Snellen, I. A. G. et al. (2010). „The orbital motion, absolute mass and high-altitude winds of exoplanet HD209458b." In: *Nature* 465, pp. 1049–1051. DOI: 10.1038/nature09111. arXiv: 1006.4364 [astro-ph.EP].

Snellen, I. A. G. et al. (2014). „Fast spin of the young extrasolar planet β Pictoris b." In: *Nature* 509, pp. 63–65. DOI: 10.1038/nature13253.

Snellen, I. et al. (2015). „Combining high-dispersion spectroscopy with high contrast imaging: Probing rocky planets around our nearest neighbors." In: *A&A* 576, A59, A59. DOI: 10.1051/0004-6361/201425018. arXiv: 1503.01136 [astro-ph.EP].

Sparks, W. B. and H. C. Ford (2002). „Imaging Spectroscopy for Extrasolar Planet Detection." In: *ApJ* 578, pp. 543–564. DOI: 10.1086/342401. eprint: astro-ph/0209078.

Sparks, W. B. et al. (2009). „Detection of circular polarization in light scattered from photosynthetic microbes." In: *Proceedings of the National Academy*

of Science 106, pp. 7816–7821. DOI: 10.1073/pnas.0810215106. arXiv: 0904.4646 [astro-ph.EP].

Sparks, W. et al. (2012). „Remote sensing of chiral signatures on Mars." In: *Planet. Space Sci.* 72, pp. 111–115. DOI: 10.1016/j.pss.2012.08.010. arXiv: 1209.0671 [astro-ph.EP].

St. John, C. E. and S. B. Nicholson (1922). „The Absence of Oxygen and Water-Vapor Lines in the Spectrum of Venus." In: *ApJ* 56, p. 380. DOI: 10.1086/142712.

Stam, D. M. (2008). „Spectropolarimetric signatures of Earth-like extrasolar planets." In: *A&A* 482, pp. 989–1007. DOI: 10.1051/0004-6361:20078358. arXiv: 0707.3905.

Stam, D. M., J. W. Hovenier, and L. B. F. M. Waters (2004). „Using polarimetry to detect and characterize Jupiter-like extrasolar planets." In: *A&A* 428, pp. 663–672. DOI: 10.1051/0004-6361:20041578.

Stevenson, K. B. et al. (2014). „Deciphering the Atmospheric Composition of WASP-12b: A Comprehensive Analysis of its Dayside Emission." In: *ApJ* 791, 36, p. 36. DOI: 10.1088/0004-637X/791/1/36. arXiv: 1406.7567 [astro-ph.EP].

Thommes, E. W., M. J. Duncan, and H. F. Levison (1999). „The formation of Uranus and Neptune in the Jupiter-Saturn region of the Solar System." In: *Nature* 402, pp. 635–638. DOI: 10.1038/45185.

Tinetti, G. et al. (2007). „Water vapour in the atmosphere of a transiting extrasolar planet." In: *Nature* 448, pp. 169–171. DOI: 10.1038/nature06002.

Todorov, K. O. et al. (2013). „Warm Spitzer Photometry of Three Hot Jupiters: HAT-P-3b, HAT-P-4b and HAT-P-12b." In: *ApJ* 770, 102, p. 102. DOI: 10.1088/0004-637X/770/2/102. arXiv: 1305.0833 [astro-ph.EP].

Tsiganis, K. et al. (2005). „Origin of the orbital architecture of the giant planets of the Solar System." In: *Nature* 435, pp. 459–461. DOI: 10.1038/nature03539.

Vidal-Madjar, A. et al. (2011). „The upper atmosphere of the exoplanet HD 209458b revealed by the sodium D lines: temperature-pressure profile, ionization layer and thermosphere (Corrigendum)." In: *A&A* 533, C4, p. C4. DOI: 10.1051/0004-6361/201015698e. arXiv: 1110.5750 [astro-ph.EP].

Wang, J. et al. (2017). „Observing Exoplanets with High Dispersion Coronagraphy. I. The Scientific Potential of Current and Next-generation Large Ground and Space Telescopes." In: *AJ* 153, 183, p. 183. DOI: 10.3847/1538-3881/aa6474. arXiv: 1703.00582 [astro-ph.EP].

Ward, W. R. (1997). „Protoplanet Migration by Nebula Tides." In: *Icarus* 126, pp. 261–281. DOI: 10.1006/icar.1996.5647.

Weidenschilling, S. J. and F. Marzari (1996). „Gravitational scattering as a possible origin for giant planets at small stellar distances." In: *Nature* 384, pp. 619–621. DOI: 10.1038/384619a0.

Whipple, F. J. W. (1931). „Meteorological conditions on Venus." In: *The Observatory* 54, pp. 86–87.

Wolszczan, A. and D. A. Frail (1992). „A planetary system around the millisecond pulsar PSR1257 + 12." In: *Nature* 355, pp. 145–147. DOI: 10.1038/355145a0.

Zellem, R. T. et al. (2014). „The 4.5 μm Full-orbit Phase Curve of the Hot Jupiter HD 209458b." In: *ApJ* 790, 53, p. 53. DOI: 10.1088/0004-637X/790/1/53. arXiv: 1405.5923 [astro-ph.EP].

Zsom, A. (2015). „A Population-based Habitable Zone Perspective." In: *ApJ* 813, 9, p. 9. DOI: 10.1088/0004-637X/813/1/9. arXiv: 1510.06885 [astro-ph.EP].